NANO LETTERS

2007
Vol. 7, No. 8
2370−2376

Magnetic Molybdenum Disulfide Nanosheet Films

Jia Zhang,[†,§] Jia Mei Soon,[†] Kian Ping Loh,[*,†] Jianhua Yin,[‡] Jun Ding,[‡] Michael B. Sullivian,[§] and Ping Wu[§]

Department of Chemistry, National University of Singapore, 3 Science Drive 3, Singapore 117543, Department of Material Science and Engineering, National University of Singapore, and Institute of High Performance Computing, Capricorn, Singapore Science Park II, Singapore 117528

Received April 30, 2007; Revised Manuscript Received June 9, 2007

ABSTRACT

Bulk molybdenum disulfide is known to be a nonmagnetic material. We have synthesized edge-oriented MoS_2 nanosheet-like films that exhibit weak magnetism (∼1–2 emu/g) and 2.5% magnetoresistance effects with a Curie temperature of 685 K. The magnetization is related to the presence of edge spins on the prismatic edges of the nanosheets. Spin-polarized calculations were performed on triangular-shaped cluster models in order to provide insight into the origin of magnetism on the edges as well as the size-property correlation in these MoS_2 nanosheets. Our results imply that nanostructured films with a high density of edge spins can give rise to magnetism even though the bulk material is nonmagnetic.

Layered transition metal disulfides like molybdenum disulfides (MoS_2) have interesting catalytic, photovoltaic, and lubricant properties.[1−3] Depending on the growth process, MoS_2 films exhibiting either edge-termination or basal-plane termination can be synthesized.[4] The edge-terminated atoms are particularly important because they play an active role in hydrodesulfurization catalysis.[5] In addition, these edge atoms can potentially exhibit unique magnetic and electronic properties that are different from the bulk.

The edge atoms on the truncated surface do not always keep the bulk stoichiometry due to changes in coordination; therefore, various types of reconstructions, as well as nonuniform spin distribution, can arise. Some forms of edge reconstructions result in Mo−Mo or S−S bonding in which the edge Mo atoms can be viewed as special Mo_xS_y clusters assembled periodically in one dimension along the edge plane. In principle, magnetic moments can arise in these Mo clusters due to partially filled d orbitals. The trigonal prismatic coordination observed for the +4 valency of Mo in bulk MoS_2, and which is responsible for spin-pairing of the d^2 electrons, may relax to octahedral coordination at the edges, leading to spin polarization of the d^2 electrons.[6] Indeed, a recent theoretical study[7] found that Mo_nS_{2n} clusters can exhibit magnetic moments, where, for example, Mo_6S_{12} has been found to be a particularly interesting molecular magnet with a large energy difference (0.94 eV) between magnetic and nonmagnetic isomers. Besides MoS_2 clusters, spin-polarized calculations on MoS_2 nanotubes suggests that the armchair structure with intercalated iodine can acquire very large spontaneous magnetic moment of 12 μ_B.[8]

So far, the only experimental report on magnetism in MoS_2 came from a study on an ensemble of weakly coupled lithium-doped MoS_2 nanotubes, where a very large, nearly temperature-independent Pauli-like susceptibility was observed.[9] However, the origin of ferromagnetic correlation for such a one-dimensional system is not understood. It appears that MoS_2 affords intriguing possibilities for observing magnetic properties through either their layered structures, which allow intercalation of foreign atoms, or through the possibilities of generating edge terminations. Recently, we found a method to prepare MoS_2 films consisting of triangular-like MoS_2 nanosheets with a high density of reactive basal edges.[10] In the past, the scientific interests on these edges focused mainly on their catalytic properties. In this paper, we provide experimental evidence that an old material like MoS_2 can have an unexpected "new" property like magnetism when rendered in the nanostructured form. To provide insight into the origin of the magnetism, which depends critically on the arrangements of Mo and S atoms at the edge, as well as the size of the nanolcusters, first-principles calculations were performed to simulate the magnetic properties.

* To whom correspondence should be addressed. E-mail: chmlohkp@nus.edu.sg.
[†] Department of Chemistry, National University of Singapore.
[‡] Department of Material Science and Engineering, National University of Singapore.
[§] Institute of High Performance Computing, Capricorn.

10.1021/nl071016r CCC: $37.00
Published on Web 07/17/2007

The Mo (4+) in bulk MoS_2 crystal adopts a trigonal-prismatic structure with respect to the six sulfur atoms around it. Because of ligand-field splitting, the d orbitals of Mo are divided into three groups, a_1', e', and e'' in trigonal prismatic coordination. The nondegenerate a_1' corresponds to d_{z^2} orbital, while d_{xy}, $d_{x^2-y^2}$ and d_{xz}, d_{yz} belong to two doubly degenerate e' and e'', respectively. Molecular orbital calculations indicated that the a_1' level is the lowest d level;[11] therefore, for $4d^2$ configuration, two d electrons will be spin-paired on the a_1' level. The spin-pairing results in diamagnetism for the MoS_2 bulk or defect-free MoS_2 (0001) surface; we have verified this through DFT calculations presented in this work.

MoS_2 thin films were prepared by thermal evaporation of the single-source precursor tetrakis(diethylaminodithiocarbomate)molybdate(IV). Detailed methods of synthesis and deposition methods have been described elsewhere.[10] The substrates used for deposition in this work were Si(100) and tantalum foil. Magnetic characterization of the hysteresis loop was performed using an alternating gradient magnetometer (AGM) (MicroMag 2900, Princeton Measurement Corporation) using a maximum field of 10 kOe in 50 Oe step increments with a sampling frequency of 1 data point per second. Other magnetic measurements were performed using the superconducting quantum interference device (SQUID) (MPMS-XL model, Quantum Design). The electrical response and magnetoresistance was investigated using the four probes built into SQUID.

Density functional theory (DFT) calculations were performed using VASP program code,[12] in which a plane-wave basis set was used. The electron−ion interaction was modeled by the projector-augmented wave (PAW) method.[13,14] The Perdew−Wang form of generalized gradient approximation (GGA) was used for the exchange and correlation functional.[15] The plane-wave cutoff energy was set to 260 eV. The Brillouin zone was sampled by $8 \times 8 \times 2$ k-point mesh for the bulk MoS_2 in the hexagonal structure. The calculated lattice constant was $a = 3.178$ Å and $c = 12.521$ Å, in good agreement with the experimental values of 3.160 and 12.584 Å,[16] respectively. The MoS_2 (0001) surface was simulated by a single-layer supercell with a c dimension of 13 Å, roughly equal to that of the bulk cell. The vacuum in c direction is large enough that there is no interaction between adjacent surfaces.[17] The S- and Mo-defect calculations have been performed using a 3×3 surface unit cell, which has been adopted by other groups to study the point defect.[18] A S vacancy defect (V_S) was simulated by removing a S atom along with two valence electrons from the top layer, likewise a Mo vacancy defect (V_{Mo}) was formed by removing a Mo atom with four valence electrons, which amounts to a defect concentration of 3.7%.

Our results show that the nanostructured form of MoS_2 can exhibit weak magnetism. Using the single-source precursor tetrakis(diethylaminodithiocarbomate)molybdate(IV) and evaporating it onto heated substrates like silicon or tantalum produced triangular-like nanosheets that terminates in sharp edges with the typical dimension of an edge measuring ~100 nm. The magnetization is sensitive to the morphology of the films. The magnetization curves with two different thicknesses and morphologies are shown in Figure 1. Typically, hysteresis loops obtained at room temperature (298 K) display saturation magnetization of ~1−2 emu/g with an applied field of 2000 Oe (1 Oe = 10^{-4} T). The absence of magnetism in MoS_2 bulk film was verified under similar testing conditions using a commercially available single-crystal molybdenite mineral, 2H-MoS_2 (99.8+%, SPI Supplies). In the SEM image shown in Figure 1, the thicker film (sample I) exhibits thicker edge-oriented sheets, while the thinner film (sample II) shows smaller-sized nanosheets with a higher density of prismatic edges. The results confirmed that a higher magnetization was measured from sample II compared to sample I. Thick films usually show a lower density of prismatic edges because of secondary nucleation on these prismatic sites. In addition, the secondary crystals increase in size, resulting in a lower surface area to volume ratio. We observed a decrease in the magnetism of the films as the mass of the material increases with deposition time, with an accompanying change in morphology and crystal size. Therefore, it is evident that the magnetization detected is not an intrinsic property of the bulk material, but rather it is due to the manisfestation of surface effects. Investigation of temperature variation of the magnetization in Figure 2a shows a Curie temperature of 412 °C (685 K). Beyond 412 °C, magnetization is nearly zero, which indicates that the magnetization is due to the intrinsic character of MoS_2 rather than contamination from metallic impurities that have a much higher Curie temperatures. Magnetic profiling was performed from room temperature to liquid helium temperature at intervals of 20 K. Figure 2b shows no significant change in magnetization at low temperatures. It is noteworthy that the Curie temperature of the MoS_2 thin films is higher (685 K) than that of magnetic semiconductors like $Co_{1-x}Fe_xS_2$ (T_C = 150 K) and CoS_2 (T_C = 121 K) and dilute magnetic semiconductors GaMnAs (T_C < 110 K) and InMnAs (T_C < 35 K). The semiconducting behavior of the MoS_2 film is demonstrated by its negative temperature coefficient, as shown in Figure 3. In addition, the magnetic MoS_2 thin films show 2.5% magnetoresistance at room temperature when subjected to a low magnetic field of >2 kOe (Figure 3, inset).

The single-source precursor used in making the MoS_2 nanosheets can also be used to fabricate MoS_2 nanotubes by thermally evaporating the precursor onto an alumina template.[19] However, the nanotubes were tested to be nonmagnetic. This suggests that the magnetism was not due to contaminants in our source because a similar source and setup were used for the fabrication of both films and tubes, but rather it is related to the intrinsic morphology of the materials. The observed magnetism is thought to originate from the high proportion of basal edges, which originates from the growth conditions that favor edge-oriented films.

To investigate the magnetic properties of the edge atoms, triangular-shaped cluster models were built in order to simulate the MoS_2 nanosheet edges. Gibbs−Curie−Wulff equilibrium morphologies reveal that a high chemical potential of sulfur leads to triangular-shaped particles

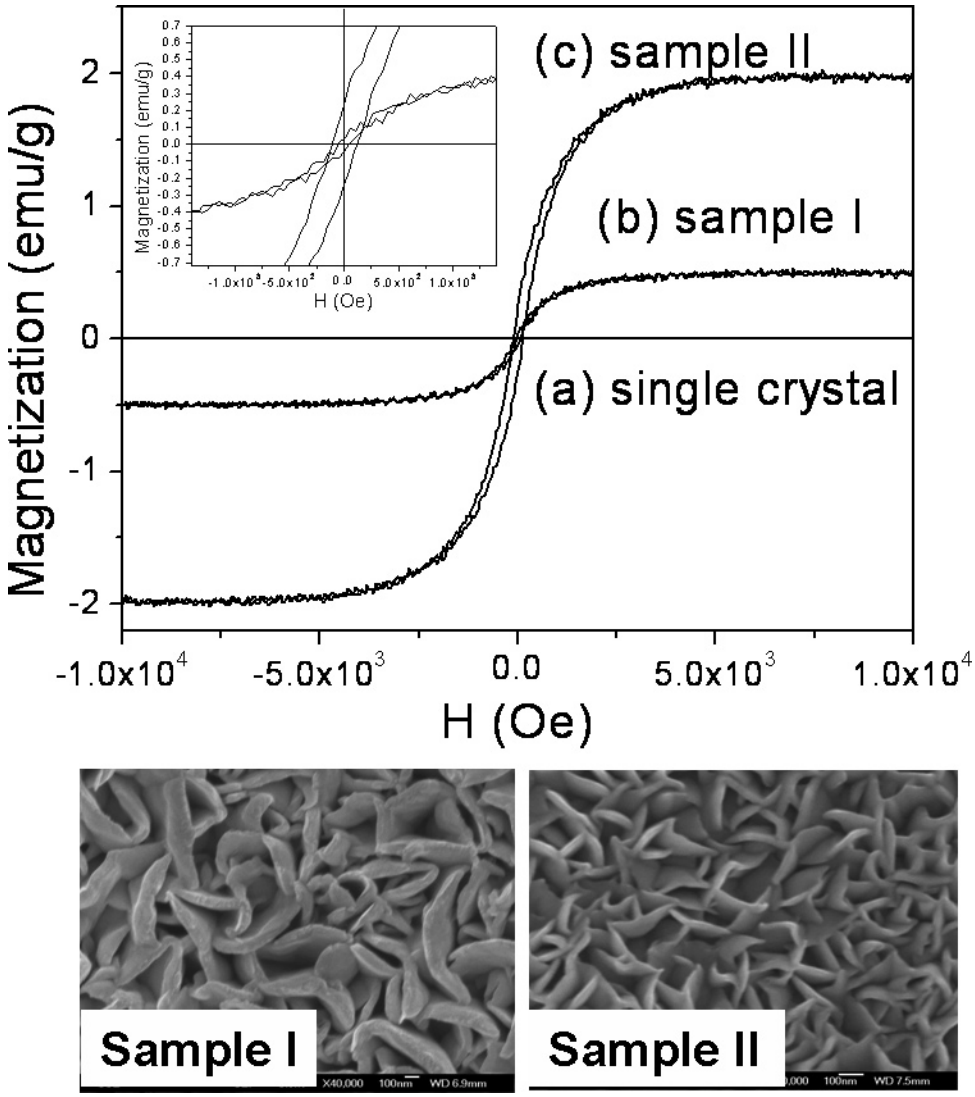

Figure 1. Hysteresis curves recorded at room temperature from two MoS_2 samples (I and II) of varying morphology (scanning electron micrographs below) using a magnetic field of 2000 Oe. The MoS_2 single crystal is nonmagnetic and shows a flat line, as indicated by the arrow.

terminated by the Mo-edge surface.[20] The advantage of these models is that they allow the edges to be entirely S- or Mo-terminated, so that the surface energy of the edges can be reliably calculated independently. The triangular MoS_2 clusters are cut from the infinite (0001) MoS_2 surface. The cluster size is controlled by n, which is the number of Mo atoms per edge of triangle. In our calculations, n was tested with values of 5, 6, 7, and 8. Parts a−g of Figure 4 displays the top view and side view of the relaxed triangular MoS_2 clusters terminated by Mo-edge $(10\bar{1}0)$ or S-edge $(\bar{1}010)$ with the cluster size of $n = 6$. Sulfur coverages of 100% and 50% for S-edges and sulfur coverages of 100%, 50%, and 0% for Mo-edge, respectively, were studied. The thermodynamic stability of selected coverages has been verified by previous theoretical calculations.[21]

In principle, there are two ways whereby spontaneous magnetism can arise for nanostructured MoS_2. First, local magnetism can arise if a high density of point defects exists. Second, if MoS_2 can be fabricated to exhibit high density of edge terminations, spontaneous magnetism may arise from the nonstoichiometry at the edge due to the different Mo:S coordination. Two types of point defects can be generated on MoS_2 (0001) with either S (V_S) or Mo vacancy (V_{Mo}). In this case, an infinite MoS_2 sheet was considered by applying periodic boundary conditions. The D_{3h} symmetry was maintained for the V_{Mo} defect, and C_{3v} symmetry was maintained for the V_S defect upon relaxation. Table 1 shows the calculated magnetic moment and the energy difference (ΔE) between the spin-polarized and spin-unpolarized state from which the stability of the magnetic state is estimated. It can be seen that the MoS_2 surface with V_S point defect is nonmagnetic, whereas the point defect V_{Mo} results in a magnetic moment of 1.22 μ_B. When a Mo atom is removed, the cation vacancy leads to a four-electron defect center, thus the magnetization caused by Mo defect is directly correlated to the holes on the six surrounding S atoms. However, V_{Mo} in the spin-polarized state is only 5 meV lower in energy than the spin-unpolarized state, this means that the V_{Mo} magnetic state is not stable and thermal excitation to the nonmagnetic state can occur at room temperature.

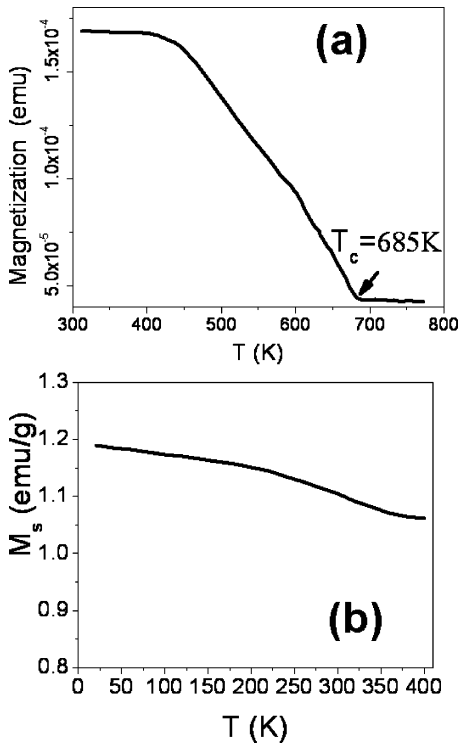

Figure 2. (a) Magnetic characterization of MoS_2 showed a Curie temperature of 412 °C with near-zero magnetization beyond this temperature. (b) The magnetization does not vary much when cooled to liquid helium temperature.

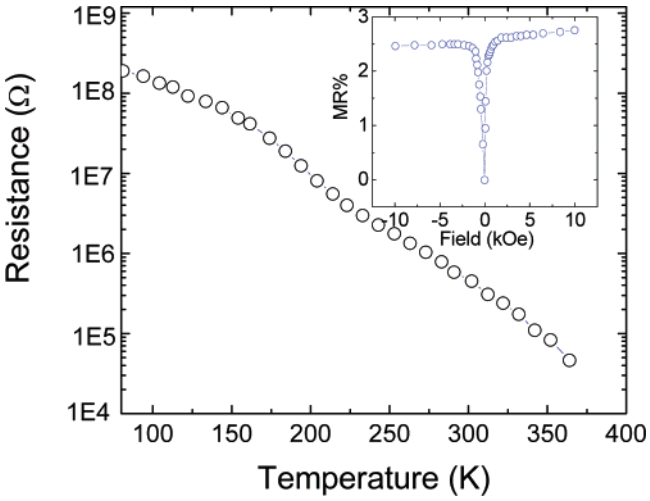

Figure 3. Change in resistance of MoS_2 with respect to temperature shows negative temperature coefficient. The inset shows 2.5% magnetoresistance exhibited by the MoS_2 thin film.

Another possibility for spontaneous magnetization arises from the edge atoms that are not fully coordinated. Table 2 shows the data for the magnetic moment and energy difference (ΔE) for triangular clusters as a function of cluster size and S coverage. S coverage on the edge can influence critically the stability of the cluster. For example, Lauritsen and Besenbacher[22] applied scanning tunneling microscope to map and classify the size-dependent structure of triangular MoS_2 nanocrystals grown on gold. They suggested that the origin of cluster size transition and "magic" cluster size may be related to the optimization of sulfur excess at the edges to have even number of sulfur dimers. In this simulation, triangular MoS_2 clusters with equilateral side consisting of either 5 or 6 atoms, i.e., $n = 5$ or 6, were studied, as shown in Figure 4. Both Mo-edged MoS_2, the $(10\bar{1}0)$ surface, and S-edged MoS_2, the $(\bar{1}010)$ surface are considered. In this study, 100% and 50% S coverage refers to 2 and 1 S atoms per Mo edge atoms, respectively. The results indicate that the Mo-edge terminated cluster without S coverage (MoS_2-Mo-0%S), and the S-edge terminated cluster with 100% S coverage (MoS_2-S-100%S) have a significant magnetic moment of 4.81 μ_B/cluster ($n = 6$) and 10.02 μ_B/cluster ($n = 6$), respectively. For MoS_2-Mo-0%S ($n = 6$), the magnetic spin isomer is 0.31 eV lower in energy than the spin-unpolarized isomer, and in the case of MoS_2-S-100%S, it is 0.55 eV lower; therefore, these magnetic states are stable. However, in the case of the Mo-edge terminated with 100% S (MoS_2-Mo-100%S) and 50% S coverage (MoS_2-Mo-50%S), as well as the S-edge terminated with 50% S coverage (MoS_2-S-50%S), there is no significant magnetic moment.

To understand how local magnetism can arise from edge Mo or S atoms, we look closely at the geometrical coordination of the edge atoms with the surrounding atoms. The following classes of atoms are distinguishable by their different bonding environment: (1) Corner atoms: Mo (or S) atoms on the three corners of the triangle are denoted by Mo_c (S_c). (2) Edge atoms: the Mo (or S) atoms on the edge of the sheet are represented by Mo_e (S_e). (3) Bulk atoms: the Mo (or S) atoms on the center away from the edges are marked by Mo_b (S_b). In parts a,b of Figure 4, the Mo edge with 100% S coverage has a capping S−S dimer after relaxation, and the outermost Mo atoms are 6-fold coordinate. The Mo atoms at the edge with 50% S coverage has capping S atoms on the bridge site and are also 6-fold coordinate. For the Mo-terminated edges that are passivated by either 50% or 100% S coverage, the edge stoichiometry is $Mo_cS_{2.7}$ and $Mo_eS_{2.3}$, respectively; in this case, the Mo edge atoms maintain the 6-fold coordination. In addition, there is also S−S bonding between S on adjacent Mo atoms to saturate the S. Therefore, no magnetism arises. However, if the Mo atoms are not passivated by any S atoms (0% S coordination), they adopt 4-fold coordination after optimization. In this case, the bond length between the Mo atoms at the corner (2.24 Å and 2.65 Å), is shorter than the bulk Mo−Mo metallic bond (2.75 Å) due to the Mo−Mo bonding. The absence of S passivation on the edge Mo (stoichiometry $Mo_eS_{1.3}$) gives rise to unpaired spins in this case, resulting in magnetism. The local magnetic moment calculation reveals that 92% of calculated magnetic moment is localized on the six edge Mo_e atoms. For larger cluster size ($n = 8$), the 78.7% and 19.8% of calculated magnetic moment is localized on the Mo_e atoms on outer ($Mo_{e(o)}$) and inner edge ($Mo_{e(i)}$) (see Figure 4e). This means that the spin polarization is not restricted only to the edge atoms at the extreme; the next nearest neighbor atoms are also influenced to have a small degree of spin polarization.

In the case of the S edge-terminated triangular clusters, the spontaneous magnetism is due to unsaturated S atoms

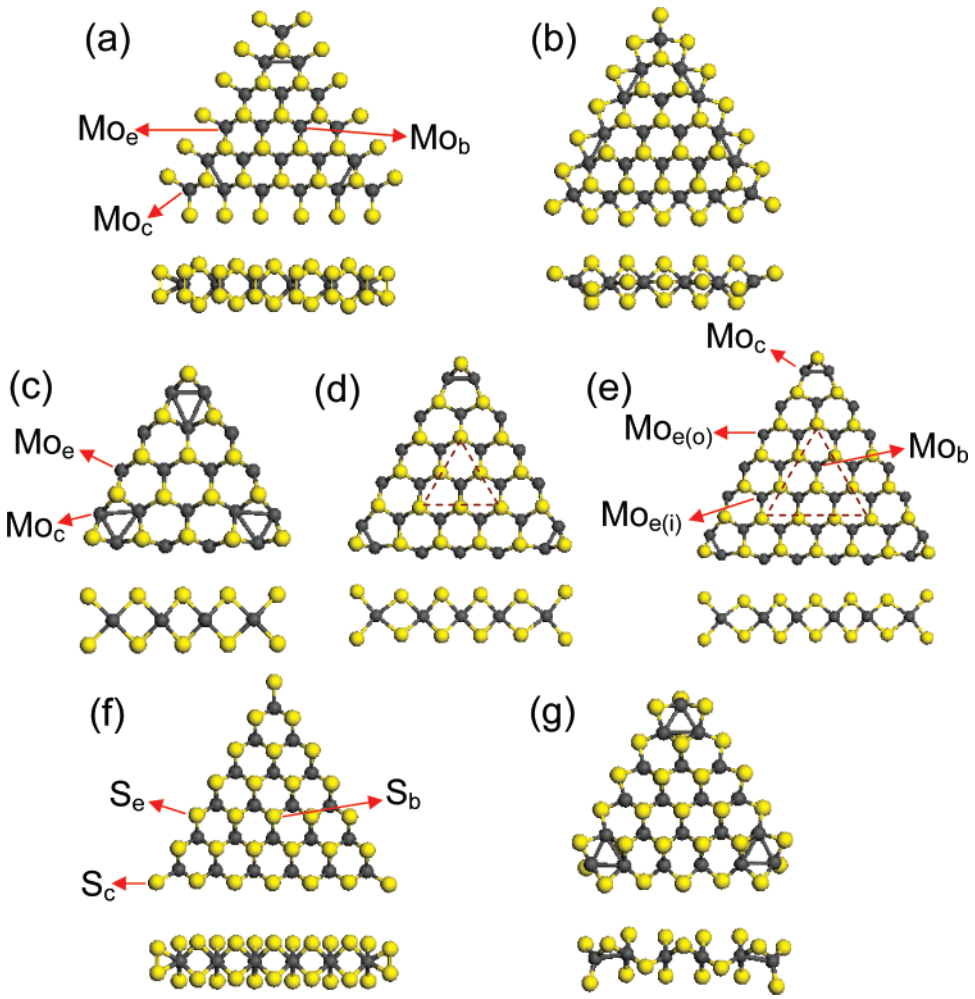

Figure 4. Top view and side view of the fully relaxed triangular-shaped MoS_2 nanosheets terminated by Mo-edge or S-edge: (a) Mo-edge with 100% S coverage ($n = 6$), (b) Mo-edge with 50% S coverage ($n = 6$), (c) Mo-edge with 0% S coverage ($n = 6$), (d) Mo-edge with 0% S coverage ($n = 7$), (e) Mo-edge with 0% S coverage ($n = 8$), (f) S-edge with 100% S coverage ($n = 6$), (g) S-edge with 50% S coverage ($n = 6$).

Table 1. Calculated Magnetic Moments and Energy Difference ΔE between Spin-Polarized and Spin-Unpolarized State for MoS_2 (0001) Surfaces with and without Vacancy Defects

	magnetic moment (μ_B)	ΔE (eV)
MoS_2 (0001)	0	0
MoS_2 (0001) (V_S)	0	0
MoS_2 (0001) (V_{Mo})	1.22	−0.005

Table 2. Calculated Magnetic Moments and Energy Difference ΔE between Spin-Polarized and Spin-Unpolarized State for Triangular-Shaped MoS_2 Clusters Terminated by S or Mo Edge

		Mo edge			S edge	
size (n)		100% S	50% S	0% S	100% S	50% S
$n = 5$	M (μ_B)	0	1.50	2.01	7.89	0.22
	ΔE (eV)	0	−0.007	−0.15	−0.37	−0.002
$n = 6$	M (μ_B)	0	0	4.81	10.02	0.33
	ΔE (eV)	0	0	−0.31	−0.55	−0.001
$n = 7$	M (μ_B)		0	9.31	12.00	0
	ΔE (eV)		0	−0.20	−0.61	0
$n = 8$	M (μ_B)			10.84	13.99	
	ΔE (eV)			−0.41	−0.72	

which passivate the S-edge. As shown in Figure 4f, the Mo atom at the edge of the S-edge triangular clusters with 100% S coverage has 6-fold coordination similar to the bulk MoS_2, spin-polarized calculations, indicating that it is not magnetic. The corner and edge Mo atoms have stoichiometric ratio of Mo_cS_3 and $Mo_eS_{2.7}$, respectively, which suggest that the excess S may be unsaturated. Indeed, dimerization of corner S atoms was also detected. Both the local magnetic moment and local density of states (LDOS) calculations verified that the spontaneous magnetization is caused by the edge- and corner-unsaturated S atoms. For the S edge that is passivated with 50% S, the stoichiometry of the Mo atoms at the corner and edge is Mo_cS_2 and $Mo_eS_{1.7}$, respectively, which is close to the bulk stoichiometry. Therefore, in this case, only very weak magnetism was detected from Mo.

In Figure 5, we present the spin LDOS of Mo-edge terminated nanosheet with 0% S coverage ($n = 8$) and S-edge terminated nanosheet with 100% S coverage ($n = 6$). The spin polarization of edge Mo and edge S atoms can be clearly observed. Figure 5a shows the S 3p and inner Mo 4d (labeled as Mo_b-4d in Figure 5a) electrons have symmetrical spin-up

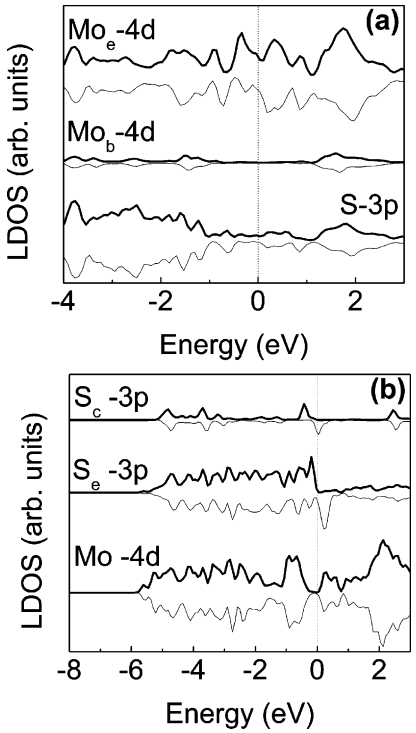

Figure 5. Local DOS for triangular-shaped MoS_2 nanosheets: (a) terminated by Mo-edge with 0% S coverage ($n = 8$); (b) terminated by S-edge with 100% S coverage ($n = 6$). The bold line indicates spin-up DOS and the lighter line indicates spin-down DOS, respectively.

and spin-down, but the edge Mo (labeled as Mo_e-4d in Figure 5a) spin-up and spin-down peaks are split asymmetrically about the Fermi level. Figure 5b shows that the 3p orbitals of edge and corner S atoms are polarized, but the Mo 4d electrons are not spin-polarized in this case. These results confirm that the magnetization of the MoS_2-Mo edge-0%S and MoS_2-S edge-100%S triangular clusters arise from the spin polarization of edge atoms Mo_e for the former, and corner S_c, and edge S_e atoms for the latter.

On the basis of the theoretical results, it can be predicted that the successful observation of macroscopic magnetism from a MoS_2 film depends on the nature of edge reconstructions. Because it is related to the edge reconstructions, a high density of such prismatic edge sites is needed to enhance the magnetic properties macroscopically. Our calculations show that the magnetic moment will increase linearly with cluster size from 6.00 μ_B when $n = 4$, to 13.99 μ_B when $n = 8$, because a bigger cluster implies a larger number of edge atoms. A plot of magnetic moment versus cluster size allows us to extract the slope, i.e., 2 μ_B per edge atom, which can be used to extrapolate the theoretical magnetization from a film with edge dimension L, consisting of n edge atoms. However, the ratio of the edge atoms normalized to the total number of atoms will decrease as the triangular cluster increases in size. The ratio of edge Mo atoms to total Mo atoms is given by $6(n - 1)/(n^2 + n)$. This implies an inverse dependence of the unit magnetic moment (magnetic moment normalized to all atoms in triangular cluster) on n, or the equivalent of a decrease in magnetization per unit gram as n increases. Therefore, a high density of small triangular clusters with a large edge atom:bulk atom ratio is needed for the weak magnetism to be detected experimentally. A triangular nanosheet with edge dimension L of 100 nm consisted of about 313 Mo atoms per edge; this will yield a magnetization of 0.44 emu/g, which is close to the experimentally measured magnetization of ~1 emu/g in this work.

The ease of deposition of these MoS_2 nanosheets by thermal evaporation on substrates affords possibilities of generating multilayer magnetic structures with possible interlayer exchange coupling. The MoS_2 nanosheet can also be intercalated with other hard magnetic materials so that higher coercivity and remanence values may be achieved. The magnetoresistance effects detected in these films implies that the alignment of spins when a magnetic field is applied results in the lowering of resistance. Although the exact explanation for this is beyond the scope of this work, it can be suggested that electrons moving in the MoS_2 nanosheet films will encounter spins at the edges that can have polarization different from that in the center. Simplistically, the resistance will be lower when excess spins in the magnetic layers are in the same direction.

In summary, we have detected weak magnetism from MoS_2 nanosheet films exhibiting a high density of prismatic edges. The magnetism arises from prismatic edge sites where the terminating atom is unsaturated. Magnetoresistance effects can arise from films consisting of such edge sites where the spin polarization is different from the bulk. The magnetic effect is correlated with the morphology of the films, and manifests most strongly for nanosheets with a high density of prismatic sites and decreases drastically when the size of the nanomaterial exceeds one micrometer. This explains why it is normally difficult to detect magnetism from the polycrystalline MoS_2 films where the crystallite size is in the micrometer range. It is possible that good size control can produce uniformly sized MoS_2 triangular clusters[22] that show unique magnetic properties. Our work indicates that metal oxides or sulfides film adopting the rhombohedral or hexagonal crystal class, and which can manifest as nanosheets with a high density of prismatic edge sites, can potentially exhibit interesting magnetic phenomena.

Acknowledgment. We thank the funding support of NUS academic grant R-143-000-221-112 for this project.

References

(1) Paskach, Y. J.; Schrader, G. L.; McCarley, R. E. *J. Catal.* **2002**, *211*, 285.
(2) Bernede, J. C.; Pouzet, J.; Gourmelon, E.; Hadouda, H. *Synth. Met.* **1999**, *99*, 45.
(3) Muratore, C.; Voevodin, A. A. *Surf. Coat. Technol.* **2006**, *201*, 4125.
(4) Jayaram, G.; Doraiswamy, N.; Marks, L. D.; Hilton, M. R. *Surf. Coat. Technol.* **1994**, *68/69*, 439.
(5) Prins, R.; De Beer, V. H. J.; Somorjai, G. A. *Catal. Rev. Sci. Eng.* **1989**, *31*, 1.
(6) Yang, D.; Jiménez Sandoval, S.; Divigalpitiya, W. M. R.; Irwin, J. C.; Frindt, R. F. *Phys. Rev. B* **1991**, *43*, 12053.
(7) Murgan, P.; Kawazoe, Y.; Ota, N. *Phys. Rev. A* **2005**, *71*, 062203.
(8) Verstraete, M.; Charlier, J.-C. *Phys. Rev. B* **2003**, *68*, 045423.
(9) Jagličić, Z.; Jeromen, A.; Trontel, Z.; Mihailović, D.; Arčon, M.; Remškar, A.; Dominko, R.; Gaberšček, M.; Martinez-Agudo, J. M.; Gómez-Garcia, C. J.; Coronado, E. *Polyhedron* **2003**, *22*, *2293.*
(10) Zhang, H.; Loh, K. P.; Sow, C. H.; Gu, H.; Su, X.; *Langmuir* **2004**, *20*, 6914.

(11) Huisman, R.; De Jonge, R.; Haas, C.; Jellinek, F. *J. Solid State Chem.* **1971**, *3*, 56.
(12) Kresse, G.; Hafner, J. *Phys. Rev. B* **1993**, *48*, 13115; **1994**, *49*, 14251.
(13) Bloechl, P. E. *Phys. Rev. B* **1994**, *50*, 17953.
(14) Kresse, G.; Joubert, D. *Phys. Rev. B* **1999**, *59*, 1758.
(15) Perdew, J. P.; Wang, Y. *Phys. Rev. B* **1992**, *45*, 13244.
(16) Weber, T.; Prins, R.; van Santen, R. A.; *Transition Metal Sulphides, Chemistry and Catalysis*; Vol. 60 of NATO Advanced Study Institute, Series 3: High Technology; Kluwer Academic Publishers: Boston, 1998.
(17) Kobayashi, K.; Yamauchi, J. *Phys. Rev. B* **1995**, *51*, 17085.
(18) Fuhr, J. D.; Saúl, A.; Sofo, J. O. *Phys. Rev. Lett.* **2004**, *92*, 026802.
(19) Loh, K. P.; Zhang, H.; Chen, W. Z.; Ji, W. *J. Phys. Chem. B* **2006**, *110*, 1235.
(20) Schweiger, H.; Raybaud, P.; Kresse, G.; Toulhoat, H. *J. Catal.* **2002**, *207*, 76Kresse, G.; Hafner, J. *Phys. Rev. B* **1993**, *48*, 13115; **1994**, *49*, 14251.
(21) Raybaud, P.; Hafner, J.; Kresse, G.; Kasztelan, S.; Toulhoat, H. *J. Catal.* **2000**, *189*, 129.
(22) Lauritsen, J. V.; Kibsgaard, J.; Helveg, S.; Topsøe, H.; Clausen, B. S.; Lægsgaard, E.; Besenbacher, F. *Nat. Nanotechnol.* **2007**, *2*, 53.

NL071016R